Pergamon

Cement and Concrete Research 29 (1999) 1561–1568

CEMENT AND CONCRETE RESEARCH

The effect of the electrochemical chloride extraction treatment on steel-reinforced mortar
Part II: Microstructural characterization

T.D. Marcotte[a], C.M. Hansson[a,*], B.B. Hope[b]

[a]*University of Waterloo, Department of Mechanical Engineering, Waterloo, Ontario N2L 3G1, Canada*
[b]*Queen's University, Department of Civil Engineering, Kingston, Ontario K7L 3N6, Canada*

Received 19 November 1998; accepted 2 June 1999

Abstract

A study has been made of the changes in cement composition and microstructures resulting from electrochemical chloride extraction applied to mortar samples in which the chlorides were added with the mixing water, ingressed by ponding with an NaCl solution, or both. After exposure for 1 year, specimens with and without chlorides were subjected to an electrochemical chloride extraction treatment. Microstructural analyses of fracture surfaces through the steel/mortar interface revealed a significant alteration of the cementitious phases. In untreated samples, calcium-silicon-rich phases consistent with Types I and II calcium silicate hydrate were observed. After the extraction treatment, these phases were not detectable and instead, sodium-rich, calcium-rich, iron-rich, and calcium-aluminum-rich phases were observed.

Keywords: Calcium-silicate-hydrate (C-S-H); Microstructure; SEM; Corrosion; Electrochemical chloride extraction

1. Introduction

The degradation of steel-reinforced concrete structures due to exposure to chlorides derived either from the use of de-icing salts or exposure to marine environments is increasing at a rate that outstrips current rehabilitation efforts. Electrochemical chloride extraction is considered as a less expensive and less time-consuming rehabilitation technique than cathodic protection. While the application of electrochemical chloride extraction has been demonstrated to remove the chloride ions from the concrete cover, thereby removing the source of the corrosion [1–3], little work has been published on the effects of the applied electric field gradient on the chemistry and microstructure of concrete in which the steel is embedded. This is essential if the practical viability of the process is to be assessed and observations of reduced bond strengths [4] and compressive strengths [5] explained. An integration of electrochemical measurements of the reinforcing steel reported in Part I [6] with the microstructural characterization of the concrete is anticipated to provide a more comprehensive understanding of the mechanisms underlying the treatment and also to provide greater insight into the future durability of treated structures.

2. Theoretical considerations

2.1. Electrochemical reactions

The application of the electrochemical chloride extraction treatment along with its associated electrochemical reactions is shown schematically in Fig. 1. The interaction of the electrochemical reactions is described in Part I of this work [6].

2.2. Effect of extraction treatment on the microstructure of concrete

There has been little published work to date presenting the effect of the extraction treatment on the chemistry and microstructure using scanning electron microscopy techniques. Most results pertaining to the microstructure have reported total porosity measurements, pore size distribution measurements, cation (Na^+, K^+, and Ca^{2+}) and chloride ion profiles, and the development of microcracks due to the extraction treatment [3,7–11]. Only Buenfeld and Broomfield [7] observed that calcium hydroxide preferentially formed at the interface during the extraction treatment.

* Corresponding author. Tel.: 519-888-4889; fax: 519-725-9971.
E-mail address: chansson@nh3adm.uwaterloo.ca (C.M. Hansson)

0008-8846/99/$ – see front matter
PII: S0008-8846(99)00117-9

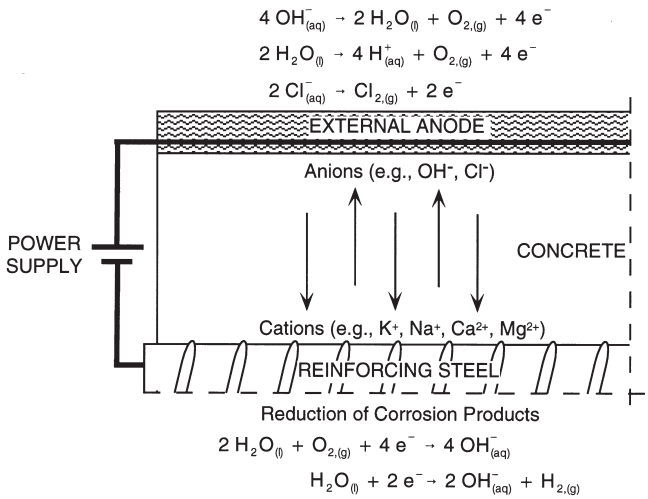

Fig. 1. Schematic illustration of the application of the electrochemical chloride extraction treatment to a corroding reinforced concrete structure.

However, a number of investigators [7,10,12,13] have reported visual changes in the concrete adjacent to the steel after an impressed current had been applied. Rosa et al. [13] observed that the first 5–10 mm of concrete adjacent to the reinforcing steel were discoloured and soft after the application of ~4.5 A/m^2 of steel for over 1 year (39370 A · h/m^2); the authors likened it to soapstone. Locke et al. [10] observed a similar effect after applying a current density of about 32 mA/m^2 for an extended period of 5 years (totalling 1415 A · h/m^2). Buenfeld and Broomfield [7] further observed that a brittle black surface layer formed over a rusty brown coloration on the steel.

3. Experimental procedures

Cylindrical mortar specimens of proportions given in Table 1 were cast with a centrally embedded steel rod (Fig. 2). These specimens were used to investigate any difference between the effect of chlorides admixed in the fresh mortar and those chlorides that ingressed into the hardened mortar from an external solution. For the admixed chlorides, 2% chlorides by mass of cement as NaCl were added to the mixing water.

Table 1
Mixture proportions and exposure regimes of the cylindrical mortar specimens

Component	Mix 1	Mix 2	Mix 3	Mix 4
Type I cement	1	1	1	1
Sand	3	3	3	3
Water	0.5	0.5	0.5	0.5
Admixed chloride ion content (percentage by mass of cement)	0	2	0	2
Ingressed chloride ion content (mol/L of immersion solution)	0	0	1	1

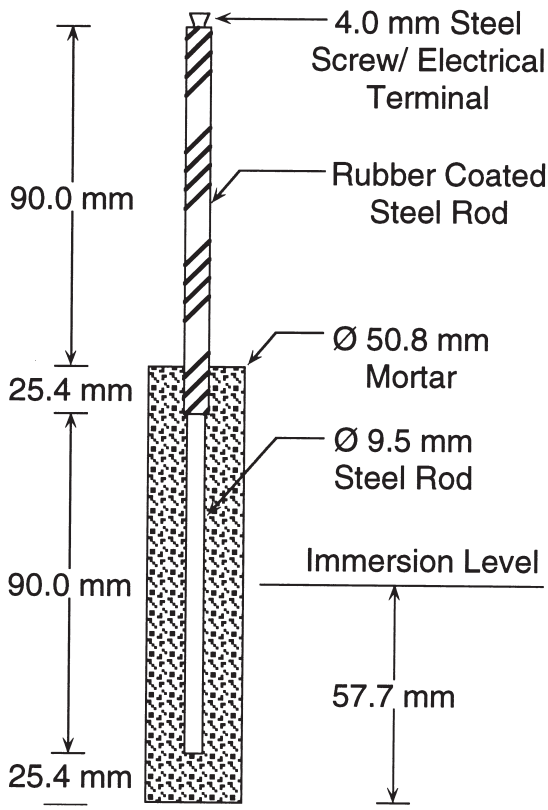

Fig. 2. Detailed drawing of cylindrical mortar specimens.

All specimens were demoulded after 24 h and cured for 28 days at approximately 25°C and 100% relative humidity. Half the specimens were immersed in a 1 M NaCl solution that was saturated with calcium hydroxide while the remainder was only immersed in a saturated calcium chloride solution. In total, four different situations were investigated and their mix proportions and exposure regimes are given in Table 1.

After approximately 10 months, an extraction treatment of 1 A/m^2 of mortar surface was applied to a representative selection of the specimens for 8 weeks using sodium borate as the electrolyte and inert titanium mesh as the external anode. Specimens that were never exposed to chlorides were also treated to investigate the effect of extraction when chlorides were absent. The remaining untreated specimens were used as controls. After 31 days immersion in a saturated calcium hydroxide solution following the extraction treatment, untreated and treated specimens were sectioned lengthwise and the steel rods were prised from the mortar. Approximately 30 mm lengths of both the steel rod and its mortar cover were further sectioned at the centre of the immersion level of the specimens indicated in Fig. 2.

The surfaces of the steel and the mortar adjacent to the steel taken from untreated and treated specimens were studied using an environmental scanning electron microscope, coupled with energy dispersive X-ray spectroscopy. Total porosity measurements and pore size distribution measure-

ments were also performed on triplicate mortar sections using mercury intrusion porosimetry. The results of these measurements are reported in other work [5].

4. Results

4.1. Fracture surfaces from untreated samples

Figs. 3(a) and 3(b) show the surface of the steel after prising from the mortar and are typical of all conditions of chloride exposure that were not subjected to the extraction treatment. These are representative of regions on the steel where fewer paste products were present which allowed the resolution of individual cementitious phases and the underlying surface of the steel to be observed. The striations on the steel surface are from the grinding of the surface of the steel rods with SiC paper before they were cast into the mortar. All surfaces had fine hexagonal plates (about 5 μm) embedded in a thin film of adherent cement paste that covered the steel. Some of the plates were half embedded within this film and EDS analyses showed that they were mainly composed of calcium. The morphology and composition indicate that these were $Ca(OH)_2$ (portlandite) crystals. The specimens that did not contain admixed chlorides [Fig. 3(a)] were more heavily covered with paste products than those containing admixed chlorides [Fig. 3(b)]. The heaviest deposit (i.e., the greatest adhesion of the paste) was on those specimens that were never exposed to chlorides.

Figs. 4(a) and 4(b) show fracture surfaces that are representative of interfacial regions of the mortar that correspond to Figs. 3(a) and 3(b). The mortar without chlorides [Fig. 4(a)] appears more textured than the mortar containing chlorides and the surface shows spherulites that have a Ca/Si ratio of about 2. These characteristics are consistent with Type I C-S-H [14]. Furthermore, rods approximately 10 μm in length were observed whose morphology and elemental constituents correspond to those of AFt [Fig. 4(a), phase A]. The mortar that contained admixed and ingressed chlorides [Fig. 4(b)] exhibited two distinct regions: the surface is either comparatively smooth [upper right area of Fig. 4(b)] or has voids of the order of 20 μm [lower left area of Fig. 4(b)]. The smooth portion of the mortar is dense with few resolvable crystals and is consistent with Type II C-S-H [14].

Figs. 5(a) and 5(b) show the paste products that remained on the surface of the steel after fracture from the mortar. All

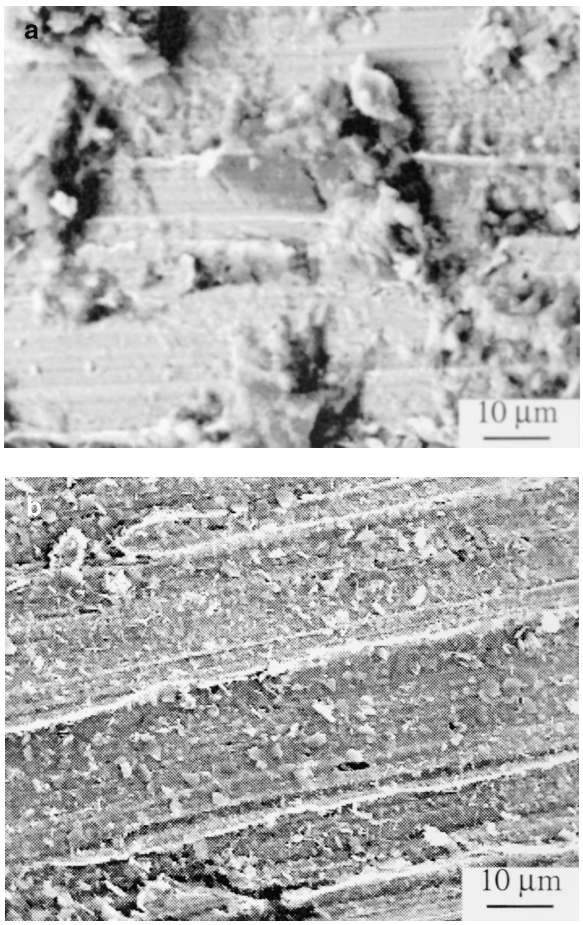

Fig. 3. (a) Steel surface from untreated sample without chlorides. (b) Steel surface from untreated sample containing admixed and ingressed chlorides.

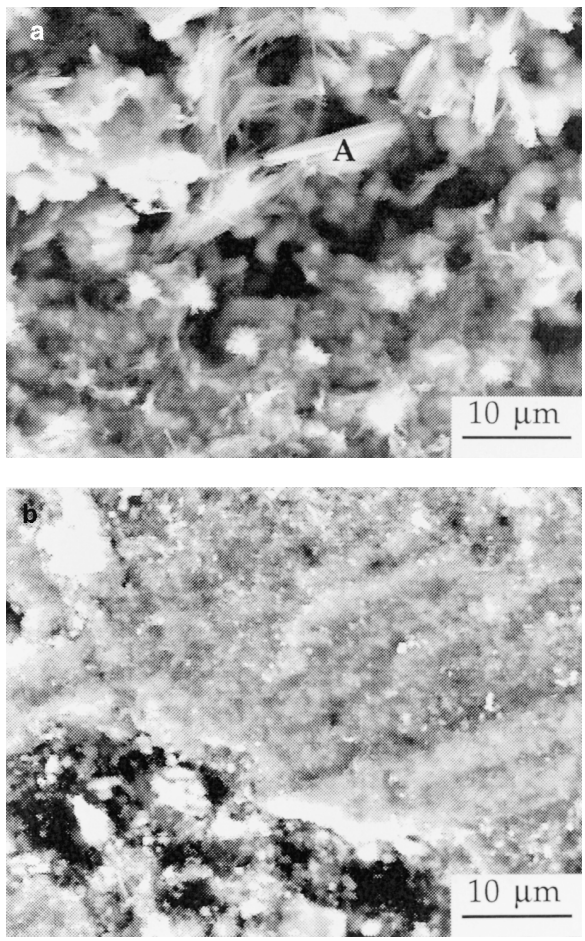

Fig. 4. (a) Mortar from untreated sample without chlorides. (b) Mortar from untreated sample containing admixed and ingressed chlorides.

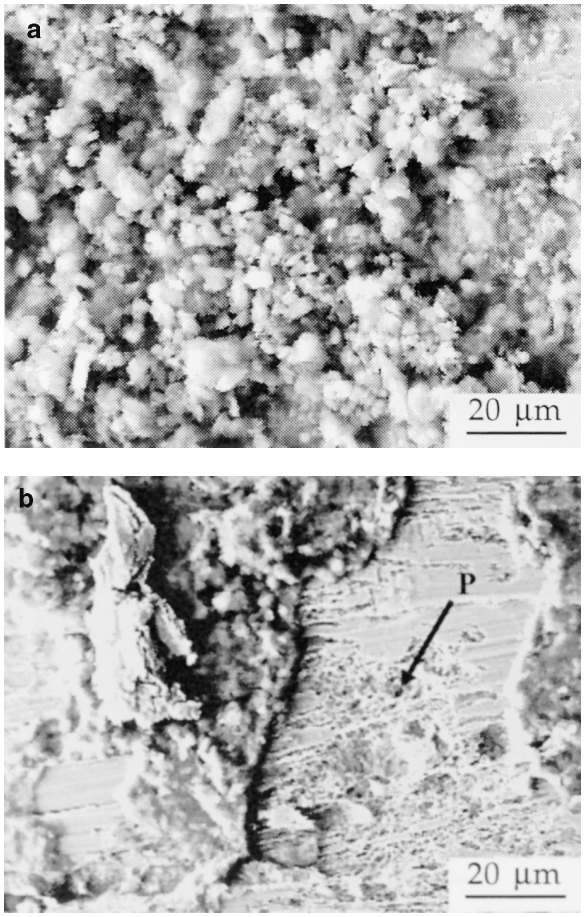

Fig. 5. (a) Steel surface from untreated sample without chlorides. (b) Steel surface from untreated sample containing admixed and ingressed chlorides.

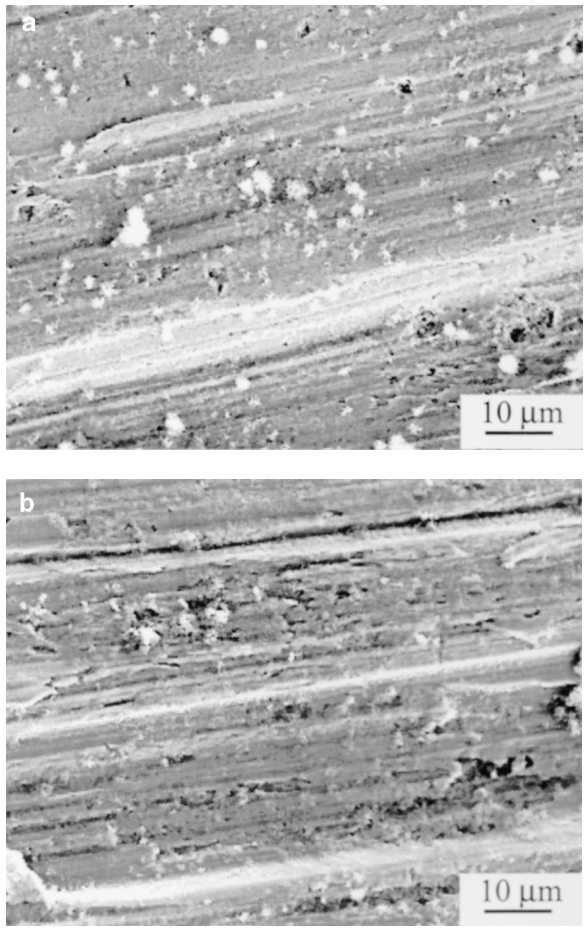

Fig. 6. (a) Steel surface from a treated sample that never contained chlorides. (b) Steel surface from a treated sample that contained admixed and ingressed chlorides.

surfaces showed products that resemble spherulite Type I C-S-H. Only the specimens that contained ingressed chlorides show characteristic chloride-induced pitting on the surface of the steel, labelled "P" in Fig. 5(b). Moreover, the regions of steel near the chloride-induced pits did not have the thin film covering that was evident in unpitted regions of the same samples [Fig. 3(b)]. Chlorides were detectable near these pits and this suggests that the film may have been spalled by the formation of corrosion products from the pitting occurring in that area, as suggested by the work of Monteiro et al. [15].

4.2. Fracture surfaces of treated specimens

Figs. 6(a) and 6(b) show the surface of the steel exposed by fracture from the mortar after the extraction treatment had ended. These regions were representative of areas where there were few paste products. The steel does not have any film over its surface (within the resolution of the microscope) and the striations in the steel were more distinct than those on the corresponding surfaces from untreated specimens. Furthermore, all of the steel samples appeared to be entirely bare in these regions except for small, white, spherical products that did not seem to be adherent to the steel.

Figs. 7(a) through 7(d) show representative regions of the steel where paste products are prevalent on the surface. A comparison of all the resulting structures after the extraction treatment showed three common features: (1) no typical C-S-H phases; (2) a local increase in calcium-aluminum-rich structures; and (3) calcium-rich hexagonal plates. The morphology that most closely resembled characteristic reticulated C-S-H [Fig. 7(a), phase B] was calcium-rich with Ca:Si ratio of approximately 7.5:1. The morphology of the calcium-aluminum-rich phase [Fig. 8, phase F] resembled calcium monosulphate (AFm) because of its crystalline, platey structure (diameters of 20–40 μm) and rosette formation, but did not contain any detectable sulphur. The third common structure was calcium-rich with a hexagonal, crystalline morphology that suggested calcium hydroxide [Figs. 7(a) and 7(c), phase C]. These plates were observed to be 15–20 μm in diameter and oriented at various angles to the surface of the steel.

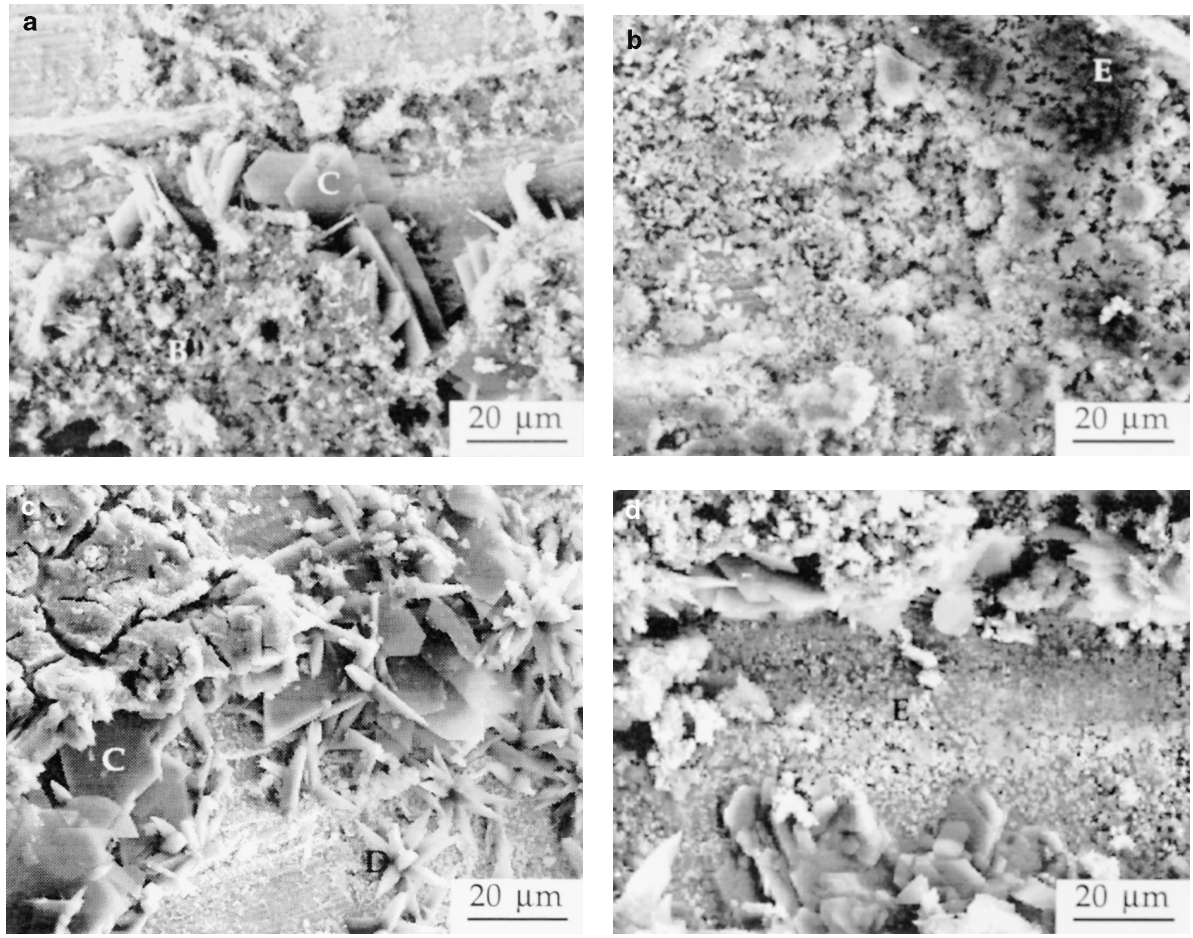

Fig. 7. (a) Paste covered steel surface from a treated sample that never contained chlorides. (b) Paste covered steel surface from a treated sample that contained admixed and ingressed chlorides. (c) Steel surface from a treated sample that contained ingressed chlorides. (d) Steel surface from a treated sample that contained admixed and ingressed chlorides.

The differences among the paste products depended on the original chloride content. A comparison of the mortar fractured from the interface shows that chloride exposure greatly diversified the number and type of paste products present. While the mortar that did not contain chlorides resembled a dense mass containing only a few hexagonal plates [Fig. 9(a)], the mortar that originally contained both admixed and ingressed chlorides had many crystalline phases [Fig. 9(b)], one of which was not observed in any other sample. This additional structure consisted of iron-rich, six-sided platelets with hexagonal symmetry. These crystals were oriented with their (0001) axis parallel to the surface of the steel and ranged in size from 5 to 30 μm in diameter (Fig. 10).

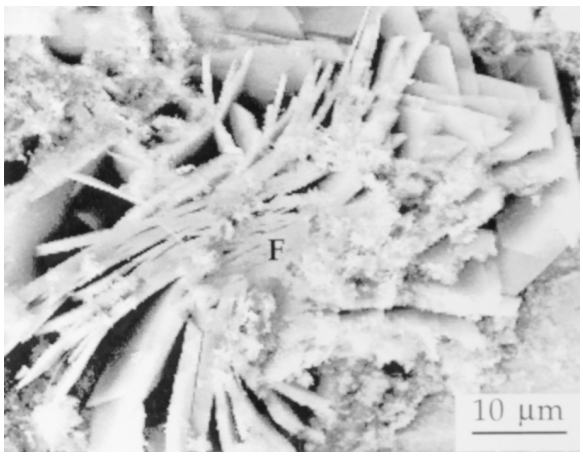

Fig. 8. Steel surface from a treated sample that never contained chlorides.

The steel from the specimen containing both admixed and ingressed chlorides was also the only sample on which calcium-aluminum rich crystals were observed in the remnants of the chloride-induced corrosion pits found on the surface of all ingressed chloride-containing specimens (Fig. 11). Chlorides were not detectable near this pit. The arrangement of these approximately 20-μm diameter plates is similar to the rosette formation of calcium-aluminum-rich plates found elsewhere on all steel samples (Fig. 8). Despite these slight differences in the crystal arrangement, these structures are likely to be the same products since the nature

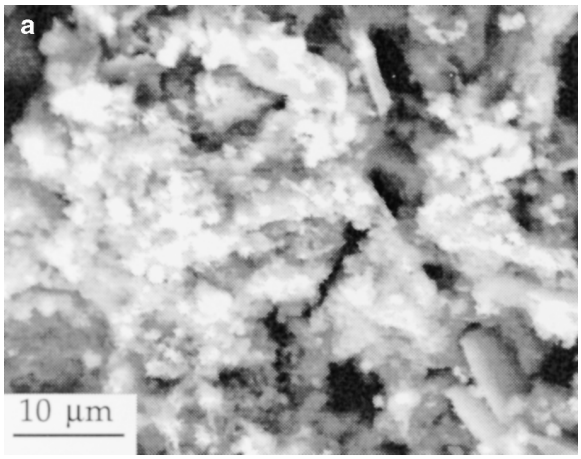

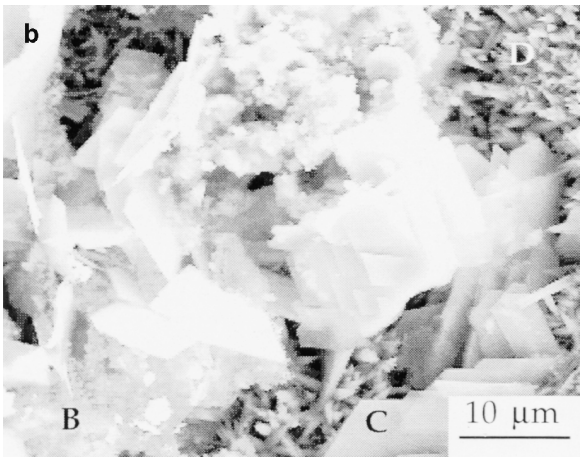

Fig. 9. (a) Mortar from a treated sample that never contained chlorides. (b) Mortar from a treated sample that contained both admixed and ingressed chlorides.

of the pit would theoretically constrain an ordered rosette formation.

Sodium-rich crystals that resembled spikes about 5 μm in length were also observed on all specimens containing chlorides [Figs. 7(c) and 9(b), phase D]. They were observed as discrete crystals but were most commonly found together resembling spiky balls or stars. In addition, the surface of the specimens that contained admixed chlorides also showed an accumulation of much smaller sodium-rich crystals [Figs. 7(b) and 7(d), phase E]. At higher magnifications these crystals appeared to be slightly gelatinous with a fine spherulite structure smaller than 2 μm.

5. Discussion

5.1. Effect of chlorides on the microstructure of mortar

For untreated samples, the morphology of the cementitious phases consistent with C-S-H depended on the type of chloride exposure. Phases identified as Type I C-S-H from their Ca/Si ratios of about 2 and a characteristic spherulite

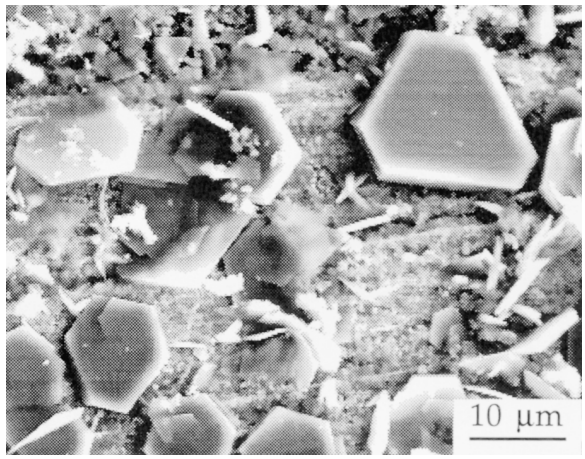

Fig. 10. Steel surface from a treated sample that contained both admixed and ingressed chlorides.

morphology were observed in the paste products for both the specimen that did not contain chlorides [Fig. 4(a)] and the specimen that contained ingressed chlorides. Alternatively, if the mortar contained admixed or admixed and ingressed chlorides, calcium-silicon-rich structures that had a reticulated morphology consistent with Type II C-S-H were observed [Fig. 4(b)]. This suggests that the early addition of sodium chlorides altered the morphology of the C-S-H hydration product in a manner similar to that observed with calcium chloride additions [16]. Pore size distribution measurements on these samples [5] also confirm a coarsening of the pores in the size range order of 0.02 μm for unexposed mortar to about 0.2 μm for mortar containing admixed chlorides. This coarsening may result from an increased C_3S hydration rate as observed on a larger scale for the addition of calcium chlorides.

The diversity of the cementitious phases observed after the extraction treatment also depended on the type of chlo-

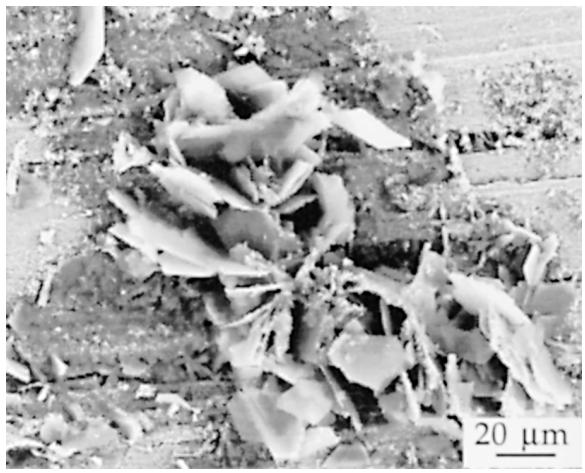

Fig. 11. Steel surface from a treated sample that contained both admixed and ingressed chlorides.

ride exposure. The formation of iron-rich plates (Fig. 10) on the steel surface from the sample that originally contained both admixed and ingressed chlorides probably resulted from the electrochemical reduction of iron corrosion products during the extraction treatment. It is probable that these plates were observed only on this type of specimen because its original, relatively high chloride content generated the most corrosion product. None of the other steel samples had as much corrosion product as this sample. Thus, the quantity of iron-rich plates formed as a result of the extraction treatment would depend on the degree of corrosion prior to the treatment.

Sodium-rich crystals forming at the interface were also only found in mortars that contained chlorides prior to the extraction treatment. Sodium-rich spiky balls were observed in all steel/mortar interfaces that originally contained chlorides either ingressed [Fig. 7(c), phase D] or admixed and ingressed [Fig. 9(b), phase D]. Only the specimens exposed to admixed chlorides were observed to contain an accumulation of much smaller, sodium-rich crystals that had a fine spherulite structure [Figs. 7(b) and 7(d), phase E]. It is possible that this structure was found in these specimens due to the larger quantities of Na^+ ions present from the admixture of the NaCl into the mortar. Hence, the sodium ions had less distance to migrate to reach the interfacial region than those samples where the ions originally ingressed from outside the sample (i.e., from the 0.1 M Na_3BO_3 electrolyte or the NaCl immersion solution).

5.2. Effect of extraction on cementitious phases

The most significant effect of extraction on the microstructure was to completely alter the chemistry and morphology of cement paste phases observable in the mortar adjacent to the steel: this effect was independent of the type of chloride exposure. Without extraction, morphologies consistent with C-S-H were detected [Figs. 4(a) and 4(b)], whereas in extracted specimens silicon was not detected in proportions significant enough to indicate the presence of C-S-H. Even those structures that resembled typical reticulated Type II C-S-H were deficient in silicon [Figs. 7(a) and 9(b), phase B].

The possible reasons for this change include: (1) the migration of calcium ions toward the steel during the extraction treatment and their incorporation into the C-S-H at the steel/mortar interface to form a structure with higher Ca/Si ratios, and/or (2) decomposition of C-S-H adjacent to the interface allowing the silicates to migrate towards the external anode. It has previously been observed that calcium ions migrate to the steel/mortar interface from the pore solution present in the "bulk" microstructure due to the extraction treatment [7]. If this migration were the only factor, the microstructure adjacent to the interface would become denser or, at least, remain at its former porosity. In the present study, the pore size distribution measurements [5] indicate a decrease in density: the porosity of inner sections of the mortar was coarsened by the extraction treatment by one to two orders of magnitude.

The fine pores measured by mercury porosimetry are considered to correspond to the finer capillary pores and, possibly, the larger gel pores within the C-S-H structure and, therefore, a decomposition of the C-S-H would lead to a restructuring and coarsening of the pores. The material generated by the decomposition might then block other larger pores, and this is supported by the decrease in coarse porosity, especially in the outer sections. The absence of silicon in the structures that resemble reticulated Type II C-S-H supports the hypothesis that silicate anions released by the decomposition and migrate to the surface of the specimen. Preliminary research on nominally 30-mm thick concrete slices using a 12-V accelerated chloride migration test has shown significant increases in the anolyte chamber of aluminum and silicon species (determined by ICP) as well as SO_4^{2-} (determined by ion chromatography) (T.D. Marcotte, C.M. Hansson, unpublished observation).

The calcium-aluminum-rich structures present in the samples after extraction (Figs. 8 and 11, phase F) may have formed by a mechanism similar to that of the calcium-rich structures with the C-S-H morphology. It has been shown experimentally that calcium aluminate hydration products preferentially form at the interface [17] and such structures were observed in Fig. 4(a) (phase A). During the hydration process, calcium aluminum trisulphate (AFt) normally decomposes to calcium aluminum monosulphate (AFm) to complete the hydration of C_3A. It then seems possible that the extraction treatment may decompose the calcium monosulphate further by removing sulphate ions but leaving a similar rosette structure, characteristic of the monosulphate. These sulphate ions might then migrate towards the external anode and react with the monosulphate to produce more trisulphate or with the C-S-H to produce gypsum. These products would contribute to the pore refinement observed in the outer sections.

The macrostructural appearance of the steel after the extraction treatment revealed that large orange-black regions had formed along with a white precipitate, as reported in Part I of this work [6]. The white precipitate may be the calcium-rich, crystalline plates (15–20 μm) observed in Figs. 7(a) and 7(c). This conclusion is based on the steel sample that was only exposed to admixed chlorides. Macrostructurally, this steel had the least amount of white precipitate on its surface and correspondingly had fewer of the calcium-rich plates observed microstructurally in Figs. 7(a) and 7(c) (phase C).

6. Summary and conclusions

The extraction treatment significantly altered the composition and morphology of the mortar at the steel/mortar interface:

- Chlorides were not detectable on the surface of the steel after the extraction treatment was performed.

- C-S-H was no longer detected after the extraction treatment possibly because it decomposed into cationic (calcium-rich) and anionic (silicate-rich) species under the impressed current.
- The proportion of calcium hydroxide increased at the interface as suggested by the macroscopic and microscopic appearance of the steel.
- New cementitious phases were formed (i.e., calcium-aluminum-rich, sodium-rich, iron-rich, and silicon-poor) and the type depended on the source and magnitude of the chloride exposure.

These microstructural observations provide an explanation for the earlier observations of discoloration of the paste and for the reduction in bond strength and compressive strength. Thus, while the electrochemical extraction process is obviously successful in removing the chlorides, it should be used with caution and practical limits of current density should be established to minimize the detrimental effects observed in the present study.

Acknowledgments

The authors would like to express their appreciation for the financial support of this work provided by the Natural Sciences and Engineering Research Council of Canada and the Ontario Centre for Materials Research.

References

[1] B. Elsener, M. Molina, H. Böhni, The electrochemical removal of chlorides from reinforced concrete, Cem Concr Res 23 (1993) 1563–1570.

[2] J. Bennett, T.J. Schue, K.C. Clear, D.L. Lankard, W.H. Hartt, W.J. Swiat, Electrochemical chloride removal and protection of concrete bridge components: Laboratory studies, Strategic Highway Research Program, National Research Council, 1993.

[3] P.F.G. Banfill, Features of the mechanism of re-alkalisation and desalination treatments for reinforced concrete, in: R.N. Swamy (Ed.), Proceedings of the Conference on Corrosion and Corrosion Protection of Steel and Concrete, Vol. 2, Sheffield Academic Press, Sheffield, UK, 1994, pp. 1489–1498.

[4] N.M. Ihekwaba, B.B. Hope, Mechanical properties of anodic and cathodic zones of ECE treated concrete, Cem Concr Res (1996) accepted for publication.

[5] T.D. Marcotte, N.M. Ihekwaba, C.M. Hansson, B.B. Hope, The effect of the electrochemical chloride extraction treatment on the microstructure and mechanical properties of cementitious materials, in: Proceedings of the Conference on Third CANMET/ACI International Symposium on Advances in Concrete Technology, V.M. Malholtra (Ed.), Auckland, New Zealand, 1997, pp. 507–529.

[6] T.D. Marcotte, C.M. Hansson, B.B. Hope, The effect of the electrochemical chloride extraction treatment on steel-reinforced mortar, Part I—Electrochemical measurements, Cem Concr Res 29 (10) (1999) 1569–1573.

[7] N.R. Buenfeld, J.P. Broomfield, Effect of chloride removal on rebar bond strength & concrete properties, in: R.N. Swamy (Ed.), Proceedings of the Conference on Corrosion and Corrosion Protection of Steel in Concrete, Vol. 2, Sheffield Academic Press, Sheffield, UK, 1994, pp. 1438–1450.

[8] J. Tritthart, K. Pettersson, B. Sørensen, Electrochemical removal of chloride from hardened cement paste, Cem Concr Res 23 (1993) 1095–1104.

[9] L. Odden, The repassivating effect of electro-chemical realkalisation and chloride extraction, in: R.N. Swamy (Ed.), Proceedings of the Conference on Corrosion and Corrosion Protection of Steel and Concrete, Vol. 2, Sheffield Academic Press, Sheffield, UK, 1994, pp. 1473–1488.

[10] C.E. Locke, C. Dehghanian, L. Gibbs, Effect of impressed current on bond strength between steel rebar and concrete, in: Proceedings of Corrosion 83, National Association of Corrosion Engineers, Anaheim, CA, USA, 1983, paper 178.

[11] J.B. Miller, Structural aspects of high powered electro-chemical treatments of re-inforced concrete, in: R.N. Swamy (Ed.), Proceedings of the Conference on Corrosion and Corrosion Protection of Steel and Concrete, Vol. 2, Sheffield Academic Press, Sheffield, UK, 1994, pp. 1499–1514.

[12] N.M. Ihekwaba, B.B. Hope, C.M. Hansson, Pull-out bond degradation of steel rebars in ECE concrete, Cem Concr Res 26 (1996) 267–282.

[13] E.B. Rosa, B. McCollum, O.S. Peters, Effect of electric currents on concrete, in: American Concrete Institute Proceedings, National Bureau of Standards, Washington, DC, USA, 1913, pp. 45–155.

[14] K.L. Scrivener, The development of microstructure during the hydration of Portland cement, Ph.D. Thesis, University of London, Imperial College, 1984.

[15] P.J.M. Monteiro, O.E. Gjørv, P.K. Mehta, Microstructure of the steel-cement paste interface in the presence of chloride, Cem Concr Res 15 (1985) 781–784.

[16] P.J. Le Sueur, D.D. Double, G.W. Groves, Chemical and morphological studies of the hydration of tricalcium silicate, Br Ceram Pro 35 (1984) 177–191.

[17] A.K. Crumbie, Characterisation of the microstructure of concrete, Ph.D. Thesis, University of London, Imperial College, 1994.